




# Eight-pass Yb:YLF cryogenic amplifier generating 305-mJ pulses

YIZHOU LIU,<sup>1,2</sup> UMIT DEMIRBAS,<sup>1,4</sup>  MARTIN KELLERT,<sup>1</sup> JELTO THESINGA,<sup>1</sup> HUSEYIN CANKAYA,<sup>1,2,3</sup>  YI HUA,<sup>1,2</sup> LUIS E. ZAPATA,<sup>1</sup> MIKHAIL PERGAMENT,<sup>1</sup> AND FRANZ X. KÄRTNER<sup>1,2,3,\*</sup> 

<sup>1</sup>Center for Free-Electron Laser Science, Deutsches Elektronen-Synchrotron DESY, Notkestraße 85, 22607 Hamburg, Germany

<sup>2</sup>Physics Department, University of Hamburg, Luruper Chaussee 149, 22761 Hamburg, Germany

<sup>3</sup>The Hamburg Centre for Ultrafast Imaging, Luruper Chaussee 149, 22761 Hamburg, Germany

<sup>4</sup>Laser Technology Laboratory, Antalya Bilim University, 07190 Dosemealti, Antalya, Turkey

\*franz.kaertner@cjel.de

**Abstract:** We report record output pulse energies from a cryogenic 8-pass Yb:YLF amplifier system operating at 10 Hz repetition rate. When seeded with 20-mJ, 1-ns stretched pulses, the amplifier produced output pulses with 305 mJ of energy at 1018.5 nm with a spectral width supporting sub-ps pulse-duration. The output beam profile was quite symmetric and had a measured beam quality factor ( $M^2$ ) of  $\sim 1.45$ . To achieve this performance, the diameter of the beam inside the gain element is gradually increased via an adjustable telescope from around 4.6 mm to 6.2 mm. This enables adjustment of the fluence to a moderate value in subsequent passes: high enough for efficient extraction and low enough to prevent laser induced damage. To our knowledge, this is the highest pulse energy reported from cryogenically cooled Yb:YLF amplifiers to date. Further scaling in peak power and repetition rate is anticipated in future work.

© 2020 Optical Society of America under the terms of the [OSA Open Access Publishing Agreement](#)

## 1. Introduction

High energy and high peak power laser amplifiers are desired in many advanced scientific applications such as optical parametric chirped-pulse amplification [1–5], high harmonic generation [6–8], high power THz generation for tabletop acceleration [9] and free-electron lasers [10]. For the past few decades, Yb<sup>3+</sup>-doped gain media have been widely used for that purpose due to their small quantum defect minimizing the heat load. Yb:YAG attracted great attention due to its long fluorescence lifetime, large emission cross section and favorable thermo-mechanical properties [11–14]. Operating Yb:YAG at cryogenic temperature turns Yb:YAG into a four-level laser and further improves its amplification efficiency and thermo-mechanical properties [15–17]. However, the gain bandwidth of Yb:YAG narrows at cryogenic temperatures significantly (full-width-half-maximum:  $\sim 1.2$  nm), leading to significant gain narrowing during the amplification process. As a result, it is quite challenging to operate cryogenic Yb:YAG systems with sub-picosecond pulse duration.

As an alternative, Yb:YLF gain media possess a broad ( $\sim 10$  nm) and rather smooth gain profile in its E//a axis at cryogenic temperatures potentially enabling generation/amplification of sub-250-fs pulses [18–24]. Moreover, when cooled with liquid nitrogen, Yb:YLF exhibits small negative thermo-optic and small thermal-expansion coefficients (pump-face bulging) leading to a small overall positive thermal lens in well designed gain-elements particularly when a bonded end-cap is used on the pump side. This can provide lower amount of beam distortion per heat load compared to Yb:YAG. Conversely, Yb:YLF has a relatively small emission cross section even at cryogenic temperatures ( $\sim 0.7 \times 10^{-20}$  cm<sup>2</sup>, which is about 4 times lower than that of room-temperature Yb:YAG). However, due to its long lifetime ( $\sim 2$  ms), one then ends up with a moderate gain amplifier medium. The saturation fluence of Yb:YLF ( $\sim 14$  J/cm<sup>2</sup>) is well above

the laser induced damage threshold (LIDT) of typical cavity optics ( $\sim 3 \text{ J/cm}^2$  for 1-ns pulses) [22], which is a drawback. As a result, compared to Yb:YAG, it is quite challenging to design efficient Yb:YLF based amplifiers, as it requires fine optimization of operation fluences for efficient extraction.

Yb:YLF has already been successfully employed in the development of high-power cryogenic lasers and amplifiers. Demirbas *et al.* achieved an output power  $> 300 \text{ W}$  with broad-tunability (995–1020.5 nm) from a continuous-wave cryogenic Yb:YLF laser [21]. In Q-switched operation, 60-ns pulses with an average power of 50 W were demonstrated at 10 kHz repetition rate [25]. By using 1-mJ seed pulses from a 10 kHz regenerative amplifier [26], Miller *et al.* demonstrated an 8-pass amplifier outputting 10-mJ pulses with 865 fs pulse duration at 10 kHz repetition rate [27]. Pulse energies up to 20-mJ with an average power as high as 70 W was achieved from a 1018 nm regenerative amplifier [20]. Working with high pulse energy and low repetition rate, Kawanaka demonstrated a regenerative amplifier producing 30-mJ pulses with 800 fs pulse duration at 20 Hz [28]. Later, Ogawa *et al.* improved the amplified pulse energy to 107 mJ by pumping harder with several diode modules in a similar amplification geometry [29]. Recently, Cankaya *et al.* further improved the output pulse energies and reported 190 mJ level pulses at 10 Hz by employing a pair of cryogenically cooled four-pass Yb:YLF amplifiers [22].

In this paper, we present up to 305-mJ of pulse energy from a compact 8-pass Yb:YLF amplifier system working at 10 Hz repetition rate. To reach this performance, an adjustable telescope was used intra-cavity, which enabled optimization of the spot size of the circulating seed for efficient extraction in subsequent passes through the gain medium. The amplified spectrum supports sub-ps pulses centered at 1018.5 nm, and the quite symmetric output beam profile was characterized with a beam quality factor below 1.5 in both axes. The system only requires a seed energy of 20 mJ, that can be directly obtained from our upgraded regenerative amplifier [20], which can enable construction of high energy Yb:YLF amplifier systems with lower-cost, smaller foot-print and improved stability. Our numerical simulations show that, the 8-pass system is also capable for high repetition rates [30].

## 2. Experimental setup

Figure 1 shows the schematic of the cryogenic Yb:YLF 8-pass amplifier that was used in our study. The system is seeded by a combination of a 1018-nm fiber front-end, a cryogenically cooled Yb:YLF regenerative amplifier and a cryogenically cooled Yb:YLF 4-pass amplifier. The 1018-nm fiber front-end delivers 15-nJ seeding pulses at 38 MHz repetition rate. The seed pulse is stretched to 1 ns by fiber Bragg gratings with a stretching ratio of  $\sim 400 \text{ ps/nm}$  [31]. The pulse energy of the stretched seed pulse is first amplified to 10 mJ inside the 10-Hz cryogenically cooled Yb:YLF regenerative amplifier. The regenerative cavity consists of a 4-mirror bowtie ring geometry with a 1.5 mm beam diameter and uses a 1.75-mm long, 25%-doped Yb:YLF crystal as the gain medium that is pumped with a 280-W, 960-nm diode [32]. The 10-mJ output beam from the regen is first expanded to a 4-mm beam diameter and then coupled to the 4-pass Yb:YLF amplifier. The cryogenically cooled 4-pass amplifier includes two 0.5%-doped Yb:YLF gain-crystals in tandem [22], and scales the pulse energy up to 140 mJ. These Yb:YLF gain elements were soldered with indium to a metal heatsink. The heatsink was then thermally contacted by compressing an indium gasket to the cooling plate of the Dewar to complete assembly, boiling liquid nitrogen in the Dewar provided primary cooling from the top. For these experiments, we directed 20 mJ of the 4-pass output to the 8-pass amplifier system instead of directing from the regenerative amplifier to avoid potential optical damages. Note that we have recently developed, in parallel, a regenerative amplifier system that can produce pulses of 25 mJ energy at up to 3 kHz [20]. Hence in future work, the 4-pass amplifier will be eliminated for further simplification of the system as is also shown in Fig. 1 with the red dashed arrow.

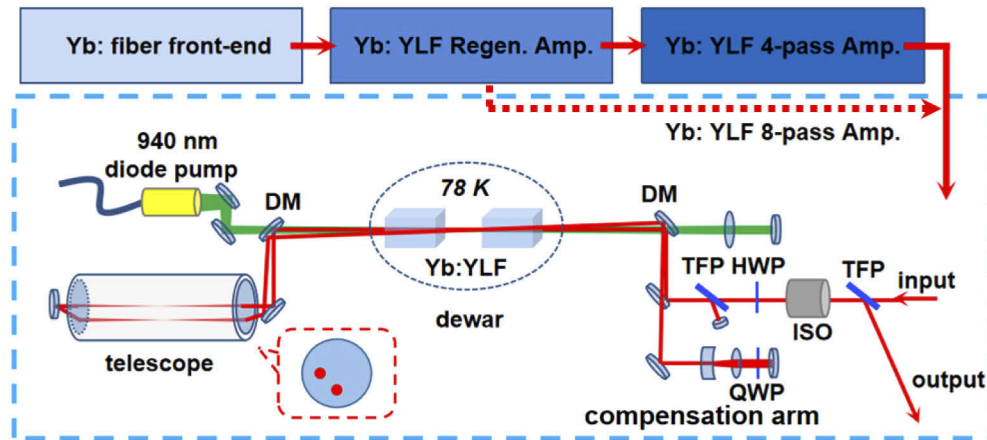


**Fig. 1.** Schematic of the cryogenically cooled Yb:YLF 8-pass amplifier system seeded by a combination of a 1018-nm Yb: fiber front-end, a Yb:YLF regenerative amplifier, and a 4-pass Yb:YLF amplifier. ISO: isolator, HWP: half waveplate, QWP: quarter waveplate, TFP: thin film polarizer, DM: dichroic mirror. Inset pattern inside the red rectangle dashed line shows the angular separation of beam paths on the lens positioned to compensate astigmatism. In the 8-pass amplifier, the two 0.5% Yb doped, 20-mm long YLF crystal are pumped from both sides by recycling the unabsorbed pump light.

The beam diameter of the amplified seed at the output port of the 4-pass amplifier is slightly enlarged from a 4 mm to 4.6-mm diameter at  $1/e^2$  and coupled into the injection line of the 8-pass amplifier consisting of a thin-film polarizer (TFP), an isolator with 12 mm aperture, a half-wave plate (HWP), a second TFP, two dichroic mirrors (DMs), and a vacuum telescope in consecutive order. Following the optical architecture prescription in Ref. [27], off-center propagation directions with  $<1^\circ$  angle are applied to realize the design of the 8-pass geometry and fulfill angularly multiplexed paths shown in the inset red rectangle dashed line inside Fig. 1. Astigmatism introduced by the off-center propagation directions can be compensated by displacing the returning beam from lens center in the orthogonal direction with respect to the incoming beam [27]. The seed pulse passes eight times through two c-cut Yb:YLF crystals in series, that are attached to a copper heat sink cooled down to 78 K by boiling liquid nitrogen. These two 20-mm Yb:YLF crystals with an aperture of  $10 \times 15$  mm have 0.5% Yb-doping concentration and 3-mm un-doped caps on both sides to minimize surface deformations. Both crystals are kept in a vacuum chamber with pressure less than  $10^{-6}$  mbar at 78 K. The E//a-axis of the Yb:YLF crystal is employed in amplification. The polarization of the seed pulse is switched between s and p-polarization by using a quarter waveplate (QWP) in the double-pass geometry, after second and sixth passes through the gain media. Therefore, the QWP works together with TFPs to realize the 8-pass geometry relying on off-center propagation directions. The thermal lens originating inside gain media is compensated after every second pass by adjusting a concave-convex telescope in the compensation arm shown in Fig. 1. The intracavity telescope consists of a -75 mm concave lens and a 100 mm convex lens. These two Yb:YLF crystals are pumped by a diode laser module providing up to 2 kW average power at 940 nm. The pump beam is delivered into the crystals via a fiber with a 600  $\mu\text{m}$  core diameter (NA 0.2) and coupled out with a telescope, mode-matching the beam into a flat-top profile with 4.14-mm beam diameter at the beam waist. The 8-pass system is pulse-pumped with 5-ms long pump pulses at 10 Hz. The unabsorbed pump beam is separated by a DM and retro-reflected back to Yb:YLF crystals. The single pass absorption of the 940 nm pump passing through the Yb:YLF gain media was measured to be around 80%, and

hence the overall pumping efficiency was estimated to be 96% for the case with the retro-reflected pump beam.

### 3. Results and discussion

Figure 2(a) shows the measured variation of the 8-pass amplifier output pulse energy with incident pump fluence. The data is taken at several different seed energy levels between 2 mJ and 20 mJ. To illustrate the benefit of double-side pumping, the data with 15 mJ seed is taken with and without the retro-reflected pump beam (15 mJ (S) indicates single side pumping). Before taking the energetics data, the telescope inter-lens separation is adjusted to over compensate the thermal lens of the Yb:YLF crystals: the incident beam diameter (4.6 mm) is expanded to acquire a 6.2 mm diameter at the output of the 8-pass amplifier while pumping the system at the full pump power (2 kW peak power, 100 W average power). Once adjusted, the inter-lens distance is kept fixed; hence at low pump fluencies, due to the smaller thermal lens, the output beam was even larger, resulting in aperture loss (since the telescope was optimized for full pump fluence configuration). We note here that the average loss per pass of the seed propagating through the 8-pass amplifier is measured as 18% (the loss observed by the seed for the cold cavity), which includes losses of the intracavity optics, as well as the aforementioned aperture losses that become minimum for the pumped cavity.

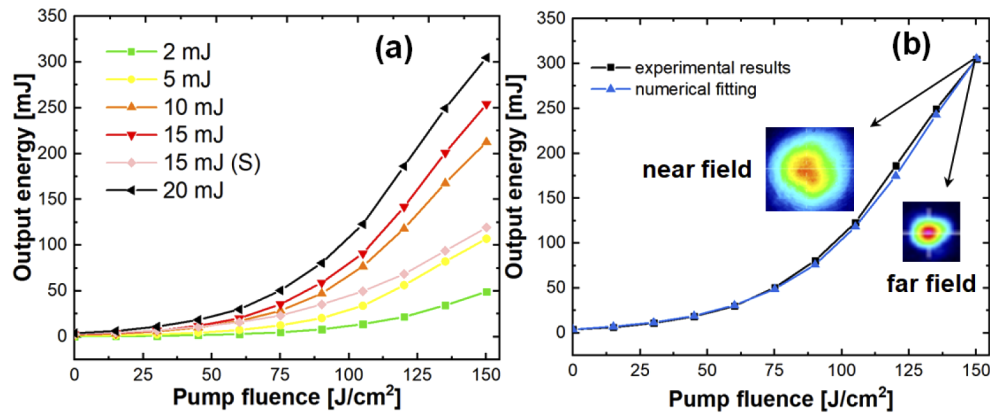
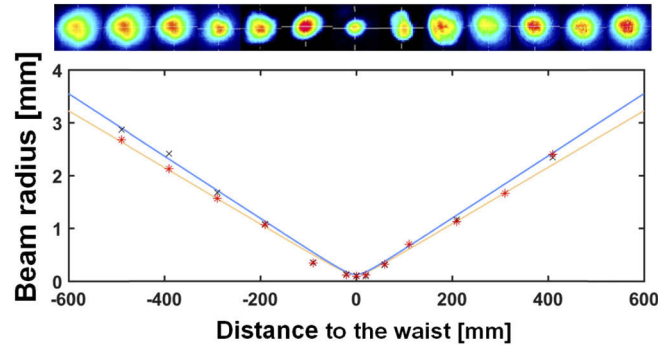


**Fig. 2.** (a) Measured variation of 8-pass amplifier output energy as a function of pump fluence at 10 Hz repetition rate, for input seed energies of 2 mJ, 5 mJ, 10 mJ, 15 mJ and 20 mJ. For the 15 mJ seed energy, single-side pumping results are also shown for comparison [15 mJ (S)]. (b) Comparison of experimental results with numerical estimations for the case with 20 mJ input seed energy. The measured near and far-field beam profiles at the maximum output energy (305-mJ) are shown as inset figures.

As shown in Fig. 2(a), for 2 mJ seed energy, the 8-pass amplifier reaches an output energy of around 50 mJ, corresponding to an overall amplification of 25. As the seed energy is increased, the system can extract better and reach higher output energies. It is instructive to compare single and dual-side pumping results data, taken for the input seed energy of 15 mJ. As one can see, retro-reflecting the unabsorbed pump back, improves the overall absorption of the pump from 80% to 96%, and increases the output energy from around 119 mJ to 254 mJ (a 16% increase in absorbed power level provides a 114% increase in output energy, clearly underlining the saturating nature of the amplifier). For the input seed energy of 20 mJ, the output of the 8-pass system reaches a record energy of 305 mJ (corresponding to an overall amplification of around 15). We have not observed any optical damage in the amplifier components, which we believe is due to the gradually increased beam diameter design that was employed in this work (will be

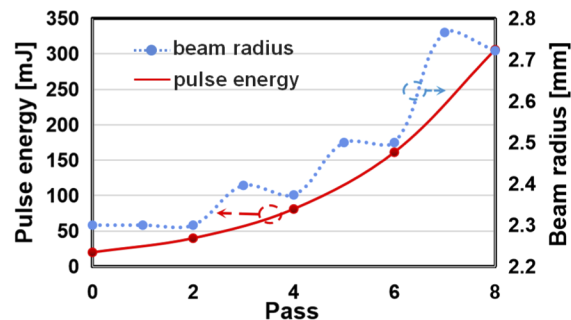
discussed in more detail later: Fig. 4). The calculated signal fluence of the 8<sup>th</sup> pass amplified pulse through the gain medium is  $2.73 \text{ J/cm}^2$ , which is slightly below the estimated damage threshold of optics for 1-ns stretched pulses ( $3 \text{ J/cm}^2$ ).

Figure 2(b) shows the measured variation of the 8-pass output energy with pump fluence for the case with 20 mJ input seed energy (black curve). The graph also shows a simple energetics calculation using the standard Frantz-Nodvik analysis [33]. A relatively good fit to the experimental data was observed (blue curve) by considering factors such as pump and seed mode-matching efficiency, and variation of seed diameter in subsequent passes. We note here that, some of the optics used such as the dichroic mirrors and Dewar windows had non-ideal passive losses for the 1020 nm wavelength, and hence the performance of the amplifier can be optimized in future studies by employing custom designed lower-loss optics. Figure 2(b) also shows measured near and far field output beam profiles at the 305 mJ energy level. As can be seen, the output beam profile was quite symmetric and had a Gaussian intensity distribution (97% fit, a further confirmation of operation of the amplifier below saturation fluence). The measured beam quality ( $M^2$  factor) of the output beam was below 1.5 in both axis, and was almost astigmatism free, confirming the good spatial quality of the system output (Fig. 3).



**Fig. 3.** Measured caustic of the 8-pass amplifier at the focus of a 500 mm focal length lens.

Earlier, we have mentioned that, the record pulse energy obtained in this study is partly due to the usage of different fluence values in subsequent passes through the amplifier. To elaborate on this issue further, Fig. 4 shows the estimated increase in pulse energy (red curve) and estimated variation in spot size (blue dashed curve) as the 20 mJ seed propagates through the 8-pass amplifier. The estimated thermal lens focal length is around 20 m for each gain crystal [20]



**Fig. 4.** Calculated variation of the energy (red curve) and radius (blue dashed curve) of the seed beam as it propagates through the 8-pass amplifier at an incident pump fluence of  $150 \text{ J/cm}^2$ .



at  $150\text{-J/cm}^2$  input pump fluence. The corresponding effective telescope focal length of the thermal lens compensation telescope is  $\sim 14\text{ m}$ . As we can see from Fig. 4, as the seed beam gets amplified, the beam radius gradually gets larger as desired, with the overall effect of thermal lensing in Yb:YLF crystals and the concave-convex telescope. This successfully avoids potential optical damage during the amplification process. The signal fluence of the 2-pass, 4-pass, 6-pass, and 8-pass amplified pulse are  $0.48\text{ J/cm}^2$ ,  $0.93\text{ J/cm}^2$ ,  $1.68\text{ J/cm}^2$ , and  $2.73\text{ J/cm}^2$ , which are lower than the damage threshold  $3\text{ J/cm}^2$  for 1-ns pulses.

Figure 5 shows the measured spectra of the seed pulse (@  $20\text{ mJ}$ ), 8-pass output (@  $305\text{-mJ}$ ) along with the emission cross section of the Yb:YLF gain medium at  $80\text{ K}$  for the E//a axis. The seed spectrum is centered around  $1018.5\text{ nm}$  and has a spectral bandwidth (FWHM) of  $2.1\text{ nm}$ . Note that, around this wavelength region the Yb:YLF gain profile has a relatively flat and smooth profile. Hence, as we can see from the amplified beam spectrum, there was a negligible gain narrowing effect during the amplification process in our study. The transform limited pulse duration corresponding to the spectrum of the amplified pulse is  $830\text{ fs}$ , and is shown as an inset to Fig. 5.

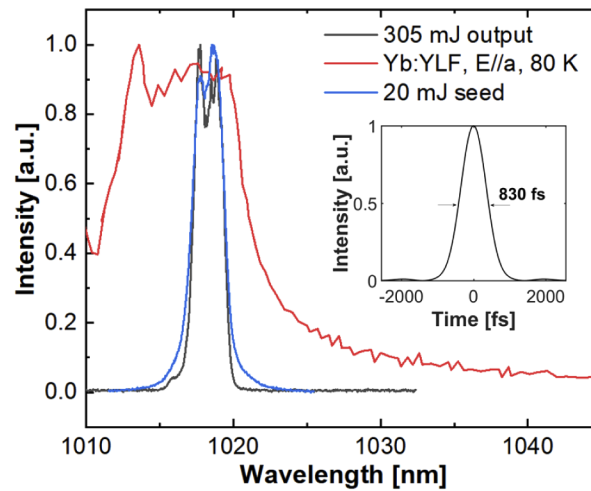


**Fig. 5.** Spectra of the amplified output pulse from the 8-pass amplifier (black curve), E//a axis emission cross section of cryogenically cooled Yb:YLF at  $80\text{ K}$  (red curve) and the  $20\text{-mJ}$  input pulse (blue curve). Inset picture shows the transform limited pulse profile of the  $305\text{-mJ}$  output pulse.

#### 4. Conclusion and outlook

In conclusion, we report a cryogenically cooled 8-pass Yb:YLF amplifier delivering  $305\text{-mJ}$  pulses. This 8-pass amplifier relies on the chirped pulse amplification architecture and uses a gradually increasing beam diameter in subsequent passes for efficient extraction of energy. This is the highest pulse energy reported from a cryogenically-cooled Yb:YLF amplifier system to date. The amplified pulse with  $2.1\text{-nm}$  spectral bandwidth centers at  $1018.5\text{ nm}$  supporting  $830\text{ fs}$  transform-limited pulse with a Gaussian pulse profile. The pulse width of the amplified pulse in our study is currently limited by the limited bandwidth of the current seed source. In future work, employing broader seed sources can eliminate this limitation and enable amplification of potentially sub- $250\text{ fs}$  level pulses. Furthermore, the system is far from saturated operation and thus, the repetition rate of the system can be further scaled up. With the aid of our Frantz-Nodvik analysis we estimate that the 8-pass system is capable of generating pulse energies above  $200\text{ mJ}$  at repetition rates of  $1\text{ kHz}$ . Such sources have great potential for applications such as pumping

of high energy and average power optical parametric amplifiers, high energy THz generation, spectral broadening & compression of high energy pulses and ultrafast X-ray generation [1–5].

## Funding

European Research Council (609920, FP7/2007–2013); Deutsche Forschungsgemeinschaft (390715994, EXC 2056); China Scholarship Council.

## Acknowledgments

The authors gratefully acknowledge the support of the engineering group, Thomas Tilp, Andrej Berg and the DESY vacuum group. Dr. Demirbas acknowledges support through a BAGEP Award of the Bilim Akademisi. Dr. Liu acknowledges partial support through funding by the China Scholarship Council.

## Disclosures

The authors declare that there are no conflicts of interest related to this article.

## References

1. J. Moses, C. Manzoni, S.-W. Huang, G. Cerullo, and F. X. Kärtner, “Temporal optimization of ultrabroadband high-energy OPCPA,” *Opt. Express* **17**(7), 5540–5555 (2009).
2. O. Chalus, P. K. Bates, M. Smolarski, and J. Biegert, “Mid-IR short-pulse OPCPA with micro-Joule energy at 100kHz,” *Opt. Express* **17**(5), 3587–3594 (2009).
3. H. Cankaya, A.-L. Calendron, C. Zhou, S. Chia, O. D. Mücke, G. Cirmi, and F. X. Kärtner, “40-μJ passively CEP-stable seed source for ytterbium-based high-energy optical waveform synthesizers,” *Opt. Express* **24**(22), 25169–25180 (2016).
4. G. Andriukaitis, T. Balčiūnas, S. Ališauskas, A. Pugžlys, A. Baltuška, T. Popmintchev, M.-C. Chen, M. M. Murnane, and H. C. Kapteyn, “90 GW peak power few-cycle mid-infrared pulses from an optical parametric amplifier,” *Opt. Lett.* **36**(15), 2755–2757 (2011).
5. G. Cerullo and S. D. Silvestri, “Ultrafast optical parametric amplifiers,” *Rev. Sci. Instrum.* **74**(1), 1–18 (2003).
6. M. Lewenstein, P. Balcou, M. Y. Ivanov, A. L’Huillier, and P. B. Corkum, “Theory of high-harmonic generation by low-frequency laser fields,” *Phys. Rev. A* **49**(3), 2117–2132 (1994).
7. P. B. Corkum and F. Krausz, “Attosecond science,” *Nat. Phys.* **3**(6), 381–387 (2007).
8. T. Popmintchev, M.-C. Chen, D. Popmintchev, P. Arpin, S. Brown, S. Ališauskas, G. Andriukaitis, T. Balčiūnas, O. D. Mücke, A. Pugžlys, A. Baltuška, B. Shim, S. E. Schrauth, A. Gaeta, C. Hernández-García, L. Plaja, A. Becker, A. Jaron-Becker, M. M. Murnane, and H. C. Kapteyn, “Bright Coherent Ultrahigh Harmonics in the keV X-ray Regime from Mid-Infrared Femtosecond Lasers,” *Science* **336**(6086), 1287–1291 (2012).
9. D. Zhang, A. Fallahi, M. Hemmer, X. Wu, M. Fakhari, Y. Hua, H. Cankaya, A. Calendron, L. E. Zapata, N. H. Matlis, and F. X. Kärtner, “Segmented terahertz electron accelerator and manipulator (STEAM),” *Nat. Photonics* **12**(6), 336–342 (2018).
10. D. A. G. Deacon, L. R. Elias, J. M. J. Madey, G. J. Ramian, H. A. Schwettman, and T. I. Smith, “First Operation of a Free-Electron laser,” *Phys. Rev. Lett.* **38**(16), 892–894 (1977).
11. P. Russbuehler, T. Mans, J. Weitenberg, H. D. Hoffmann, and R. Poprawe, “Compact diode-pumped 1.1 kW Yb:YAG Innoslab femtosecond amplifier,” *Opt. Lett.* **35**(24), 4169–4171 (2010).
12. S. Banerjee, K. Ertel, P. D. Mason, P. J. Phillips, M. Siebold, M. Loeser, C. Hernandez-Gomez, and J. L. Collier, “High-efficiency 10 J diode pumped cryogenic gas cooled Yb:YAG multislabs amplifier,” *Opt. Lett.* **37**(12), 2175–2177 (2012).
13. P. Lacovara, H. K. Choi, C. A. Wang, R. L. Aggarwal, and T. Y. Fan, “Room-temperature diode-pumped Yb:YAG laser,” *Opt. Lett.* **16**(14), 1089–1091 (1991).
14. J. Fischer, A.-C. Heinrich, S. Maier, J. Jungwirth, D. Brida, and A. Leitenstorfer, “615 fs pulses with 17 mJ energy generated by an Yb:thin-disk amplifier at 3 kHz repetition rate,” *Opt. Lett.* **41**(2), 246–249 (2016).
15. D. J. Ripin, J. R. Ochoa, R. L. Aggarwal, and T. Y. Fan, “165-W cryogenically cooled Yb:YAG laser,” *Opt. Lett.* **29**(18), 2154–2156 (2004).
16. L. E. Zapata, S. Schweisthal, J. Thesinga, C. Zapata, M. Schust, Y. Liu, M. Pergament, and F. X. Kärtner, “Joule-class 500 Hz Cryogenic Yb:YAG Chirped Pulse Amplifier,” in *Conference on Lasers and Electro-Optics*, paper SM4E. 1. (2019).
17. K.-H. Hong, A. Siddiqui, J. Moses, J. Gopinath, J. Hybl, F. Ö. Ilday, T. Y. Fan, and F. X. Kärtner, “Generation of 287 W, 5.5 ps pulses at 78 MHz repetition rate from a cryogenically cooled Yb:YAG amplifier seeded by a fiber chirped-pulse amplification system,” *Opt. Lett.* **33**(21), 2473–2475 (2008).

18. J. Kawanaka, S. Tokita, H. Nishioka, M. Fujita, K. Yamakawa, K. Ueda, and Y. Izawa, "Dramatically improved laser characteristics of diode-pumped Yb-doped materials at low temperature," *Laser Phys.* **15**, 1306–1312 (2005).
19. T. Y. Fan, D. J. Ripin, R. L. Aggarwal, J. R. Ochoa, B. Chann, M. Tilleman, and J. Spitzberg, "Cryogenic Yb<sup>3+</sup>-Doped Solid-State Lasers," *IEEE J. Sel. Top. Quantum Electron.* **13**(3), 448–459 (2007).
20. U. Demirbas, H. Cankaya, Y. Hua, J. Thesinga, M. Pergament, and F. X. Kärtner, "20-mJ, sub-ps pulses at up to 70 W average power from a cryogenic Yb:YLF regenerative amplifier," *Opt. Express* **28**(2), 2466–2479 (2020).
21. U. Demirbas, H. Cankaya, J. Thesinga, F. X. Kärtner, and M. Pergament, "Efficient, diode-pumped, high-power (>300W) cryogenic Yb:YLF laser with the broad-tunability (995–1020.5 nm): investigation of E//a-axis for lasing," *Opt. Express* **27**(25), 36562–36579 (2019).
22. H. Cankaya, U. Demirbas, Y. Hua, M. Hemmer, L. E. Zapata, M. Pergament, and F. X. Kärtner, "190-mJ cryogenically-cooled Yb:YLF amplifier system at 1019.7 nm," *OSA Continuum* **2**(12), 3547–3553 (2019).
23. I. Tamer, S. Keppler, M. Hornung, J. Körner, J. Hein, and M. C. Kaluza, "Spatio-Temporal Characterization of Pump-Induce Wavefront Aberrations in Yb<sup>3+</sup>-Doped Materials," *Laser Photonics Rev.* **12**(2), 1700211 (2018).
24. U. Demirbas, J. Thesinga, H. Cankaya, M. Kellert, F. X. Kärtner, and M. Pergament, "High-power passively mode-locked cryogenic Yb:YLF laser," *Opt. Lett.* **45**(7), 2050–2053 (2020).
25. N. Ter-Gabrielyan, V. Fromzel, T. Sanamyan, and M. Dubinskii, "Highly-efficient Q-switched Yb:YLF laser at 995 nm with a second harmonic conversion," *Opt. Mater. Express* **7**(7), 2396–2403 (2017).
26. D. Rand, D. Miller, D. J. Ripin, and T. Y. Fan, "Cryogenic Yb<sup>3+</sup>-doped materials for pulsed solid-state laser applications [invited]," *Opt. Mater. Express* **1**(3), 434–450 (2011).
27. D. E. Miller, L. E. Zapata, D. J. Ripin, and T. Y. Fan, "Sub-picosecond pulses at 100 W average power from a Yb:YLF chirped-pulse amplification system," *Opt. Lett.* **37**(13), 2700–2702 (2012).
28. J. Kawanaka, K. Yamakawa, H. Nishioka, and K.-I. Ueda, "30-mJ, diode-pumped, chirped-pulse Yb:YLF regenerative amplifier," *Opt. Lett.* **28**(21), 2121–2123 (2003).
29. K. Ogawa, Y. Akahane, and K. Yamakawa, "100-mJ diode-pumped, cryogenically-cooled Yb:YLF chirped-pulse regenerative amplifier," *CLEO:2011 – Laser Science to Photonic Applications*, Baltimore, MD, 1–2 (2011).
30. U. Demirbas, H. Cankaya, M. Pergament, and F. X. Kärtner, "Power and energy scaling of rod-type cryogenic Yb:YLF regenerative amplifiers," *J. Opt. Soc. Am. B* **37**(6), 1865–1877 (2020).
31. Y. Hua, W. Liu, M. Hemmer, L. E. Zapata, G. Zhou, D. N. Schimpf, T. Eidam, J. Limpert, A. Tünnermann, F. X. Kärtner, and G. Chang, "87-W 1018-nm Yb-fiber ultrafast seeding source for cryogenic Yb:yttrium lithium fluoride amplifier," *Opt. Lett.* **43**(8), 1686–1689 (2018).
32. M. Hemmer, L. E. Zapata, Y. Hua, and F. X. Kärtner, in *Lasers Congress 2016 (ASSL, LSC, LAC)*, OSA Technical Digest (online) (Optical Society of America, 2016), AT4A.3.
33. L. M. Frantz and J. S. Nodvik, "Theory of Pulse Propagation in a Laser Amplifier," *J. Appl. Phys.* **34**(8), 2346–2349 (1963).